Liquid phase combustion of iron in an oxygen atmosphere

Maryse Muller · Hazem El-Rabii · Rémy Fabbro

Abstract In this article, we report an investigation of laser-initiated ignition of pure iron rods, using optical pyrometry, video observations, and analysis of metallographic cross section of quenched burning liquid on copper plates. When ignition occurs, caused by the melting of metal, the combustion takes place in the liquid. Two distinct superposed phases (L1 and L2) are identified in the liquid, according to the known phase diagram of the iron oxide system. Our observations show that the L1 and L2 phases can be either distinct and immiscible or mixing together. The temperature of the transition at which the mixing occurs is around 2350 K. Two mechanisms are proposed to explain the mixing occurring at high temperature: the spontaneous emulsification resulting from a strong decrease of the interfacial tension between L1 and L2 and the reduction of the miscibility gap between them at high temperature. Based on the experimental data of the evolution of the temperature and the video observation of the melt for different ignition conditions, we provide a complete description of the combustion process of iron induced by laser. Eventually, an extrapolation of the iron–oxygen phase diagram, to temperatures higher than 2000 K, is proposed.

M. Muller (✉) · R. Fabbro
Laboratoire PIMM, CNRS/Arts et Métiers ParisTech, 151 bd.de l'Hôpital, 75013 Paris, France
e-mail: maryse.muller@ensam.eu

M. Muller
Air Liquide, CRCD, 1 chemin de la porte des Loges, les Loges en Josas, Jouy-en-Josas, France

M. Muller · H. El-Rabii
Institut Pprime, CNRS/ENSMA, 1 av. Clément Ader, BP 40109, 86961 Futuroscope Chasseneuil Cedex, France

Introduction

The idea that iron, when subjected to high temperatures in a high concentration of gaseous oxygen and/or high pressure, undergoes a liquid phase combustion process is widely accepted, [10–12, 26, 29–33, 35]. Since the oxidizer (gaseous oxygen) and the fuel (liquid iron) involved in iron combustion are present in different phases, the combustion of metals is usually qualified as "heterogeneous" contrary to the combustion of gases, qualified as "homogenous." However, the argument between Steinberg et al. and Glassman [8, 32, 33] shows that this distinction alone is insufficient to give full account of the possible complexity of the processes that may take place in the liquid.

In particular, questions related to the exact location of the combustion in the melt, the composition of the melt, and the rate-limiting mechanism of combustion are still open. Concerning the location of the reaction, very first investigation by Harrison suggests that iron and iron alloys do not burn in vapor phase, but that "the reaction takes place at the surface of [the] molten mixture" [9]. This assertion is based on the observation of a "variation of the position of a dark zone" on the liquid drop, leading the authors to conclude that the composition of the liquid surface may vary from pure liquid iron to iron oxide. The exact composition of the molten mixture and the rate-limiting mechanism of the combustion were not addressed.

Further experimental work conducted by Sato et al. on mild steel rods shows similar variations in the brightness on the liquid surface [28]. Using high-speed photography, they notice that the movements in the liquid are about few tens of cm/s, and directed from more to less oxidized liquid, and they infer that convection would be the dominant mode of heat transfer at the molten/solid interface. Analyzing the movement of the drop, they also determine

that the liquid drop would be mostly composed of liquid iron oxide, and that the oxidation reaction should thus take place within the molten metal oxide mass. The same idea is further developed by Hirano and co-workers [10–12]. They deduced from the relation between the mean regression rate of the rod and the oxygen pressure that the rate-limiting mechanism is either the physical adsorption, or the chemical adsorption or the incorporation of oxygen at the oxygen–oxide interface. Similar observations made by Ohtani [23] and then by Sato et al.[27] for the ignition of massive iron blocks even lead them to infer that the convection was essential in the combustion process. Steinberg *et al*., observing the movements of the dark zones on the surface of the liquid during the combustion of iron rods in microgravity, concluded then that the circulation in the liquid *is* the dominant process involved in the combustion of iron [29].

In later works, Steinberg et al. [30, 31] quenched burning pure iron rods in water and observed that the resolidified ball could be divided in two distinct parts: one composed of unreacted iron and another composed of iron oxide. They therefore suggested that the molten material may be composed of an unreacted liquid iron phase in contact with solid iron, covered by a liquid iron oxide phase in contact with gaseous oxygen. Their suggestion is supported by the commonly admitted iron–oxygen phase diagram under atmospheric pressure [15, p. 109], stating the existence of two immiscible liquid phases L_1 (iron containing up to 0.2 % oxygen at 1810 K and up to 0,85 % at 2223 K [3]) and L_2 (iron oxide with oxygen content from 22.6 to more than 28 % at 1873 K [24]). Steinberg et al. also showed [30, 31], using appropriate pressure measurements in a pressure vessel where combustion of pure iron rods was taking place, that the liquid oxide phase contained an 'excess' of oxygen compared to stoechiometric proportion required to form the highest stable solid iron oxide (hematite Fe_2O_3) [31]. This leads them to infer that the rate-limiting mechanism cannot be the incorporation of oxygen as previously proposed by Hirano et al. [12], but that the reaction at the liquid iron–liquid iron oxide interface is.

The two explanations given above are clearly contradictory. Dreizin attempted to resolve the contradiction by pointing out that the gas pressure and the gas temperature may be different in each case, and that both explanations may be correct depending on the experimental conditions [4]. However, complementary experimental data are necessary to resolve this contradiction.

Indeed, high temperature is reached during the combustion of iron in gaseous oxygen, typically more than 2100 K without oxygen flowing [9, 16, 26]. The lack of reliable data concerning the existing phases at these temperatures makes the understanding of the combustion process particularly challenging. The issues of the size of the area where the reaction takes place, the chemical composition of the melt, the existence of one or two phases, their degree of miscibility, as well as the subsequent interfacial phenomena that could occur in the L1/L2 contact area are essential in the comprehension of the mechanisms involved.

In this article, we intend to respond to the question raised by the contradiction between the work reported by Sato et al. and the work of Steinberg et al. dealing with the chemical composition of the melt and the possibility for liquid iron and liquid iron oxide to mix during combustion.

We give experimental evidences that show the existence of a threshold temperature at 2350 K above which, during the combustion of iron, liquid iron (L1) and liquid iron oxide (L2) mix.

Moreover, we show that this threshold temperature is well above the range of temperatures usually represented in the phase diagram of the iron-oxygen system (usually 2000 K), and can be represented as a reduction of the (L1+L2) area at high temperatures resulting in the merging of L1 and L2 into one unique phase. We propose then physico-chemical mechanisms to explain this phenomenon.

To achieve this goal, 3-mm-vertical diameter rods were ignited on their upper part using a focused laser beam, providing thus a very repeatable, controllable, contactless, and localized source of energy. All the experiments were made in a pure oxygen atmosphere, under ambient atmospheric pressure. Appropriate instrumentation was used to measure the temperature in the liquid and to observe the surface of the burning liquid.

The paper is organized as follows. In "Experimental set-ups" section, the experimental set-up is described. An analysis of the experimental results is made in "Experimental results" section, where video observations, temperature measurements, and metallurgical cross sections will be detailed. A discussion of these results is made in "Discussion" section, addressing the issues of the composition of the melt, the miscibility of the liquid phases, and proposing a comprehensive description of the combustion process. Finally, "Conclusions" section summarizes our conclusions.

Experimental set-ups

A schematic of the experimental set-up for laser ignition of the metal rods is shown in Fig. 1. The samples were cylindrical extra-pure iron (Goodfellow, FE007925, purity 99.99 %) rods of 15–25 mm in length and 3 mm in diameter. The surface of the rod was treated with rough sand paper (#180), in order to ensure a sufficient and repeatable absorptivity to laser radiations. They were fixed in a small

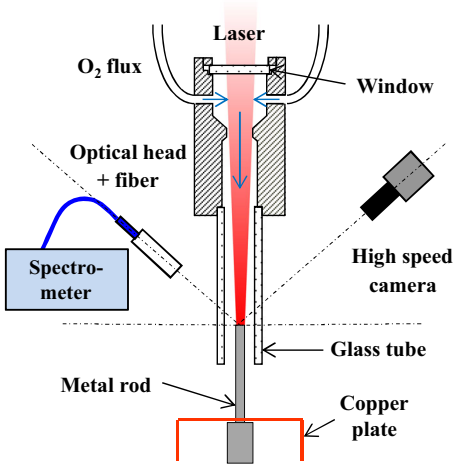

Fig. 1 Test apparatus with the optical pyrometry experimental set-up

chuck and partly placed inside a borosilicate glass tube (with an inner diameter of 16 mm), transparent to radiation in the wavelength range from 500 to 1000 nm. Oxygen gas (Air Liquide, minimum purity 99.5 %) flowed out through the glass tube (at a flow rate of 40 l/min), providing an oxidizing atmosphere to sustain their combustion. The dynamic pressure applied on the top of the rod was not strong enough to push the liquid downwards.

The metal rods were heated by a disk laser (TRUMPF TruDisk 10002) operating at 1030 nm. The laser beam was delivered through an optical fiber with a core diameter of 600 μm, providing a uniform intensity distribution that was imaged onto the top of the rod by a set of two lenses. The circular beam spot size so obtained was 3.1 mm in diameter, which ensured a homogeneous heating of the top surface of the rod. Intensities from 40 to 250 MW m^{-2} (corresponding to laser power from 320 W to 2 kW) with pulse durations from 5 ms to 1 s were used to ignite.

Two different pyrometers were used for measurement of the surface temperature of the rod during ignition and combustion: a 2D single-band pyrometer (Photron Ultima 1024 high-speed video camera with CMOS sensors and a frame rate up to 4 kHz, in the wavelength range 800–950 nm) and a spectral pyrometer (Ocean Optics USB 2000+ spectrometer used in the wavelength range from 500 to 700 nm, with a recording rate up to 500 Hz, and spectral resolution of approximately 0.9 nm).

The emissivity of liquid iron as well as that of liquid iron oxide for the calculation of temperature (2D monoband pyrometer) is considered independent of the wavelength (gray body assumption) and independent of temperature. This is justified by the fact that the range of wavelength is narrow enough (800–950 nm). Krishnan et al. [14] report values of the emissivity of pure iron at 1890 K between 0.37 and 0.35 for 800–950 nm (their work) or 0.345 and 335 for 800–950 nm (data from Cezairlyan, from private communication to Krishnan, cited in [14]). We took 0.35 (±5 %) for the emissivity of liquid iron (L1 phase). Concerning the emissivity of liquid iron oxide (L2 phase), we experimentally determined 0.7 (±10 %) for the wavelength 1064 nm, inferring this value from absorptivity measurement of liquid iron oxide of laser radiations at 1064 nm, using Kirchhoff law [18]. We also determined the same mean value of 0.7 (±15 %) in the range of wavelengths 500–700 nm using the spectral pyrometer (without any gray body assumption). We assumed then that the emissivity of the L2 phase in the range of wavelength between 600 and 1064 nm (and therefore 800–950 nm) is 0.7 (±15 %).

The spectral pyrometer used here takes into account the possible dependence of the emissivity on wavelength (assumed to be linear) and its variation through temperature changes, and does not require any gray body assumption. The temperature is deduced from the spectra acquired by the spectrometer using a suited algorithm that discriminates the part of the variations of the spectral luminance due to an emissivity variation with the wavelength from those due to a temperature change. Independent and simultaneous measurement of both temperature and emissivity are obtained and provide accurate values of the temperature, despite a poor knowledge or unexpected variations of emissivity. The uncertainty on the temperature and emissivity measurements is inferred from the uncertainty generated by the calibration process. The uncertainty on temperature determined with the spectral pyrometer is ±60 K and that on emissivity is ±15 %.

More detail on these pyrometers, their calibration, and the original simultaneous use of them can be found in detail in [20].

The Photron camera was also used to provide video recordings of the combustion in the visible and infrared region.

The camera, the spectrometer, and the laser were triggered by the same signal, ensuring synchronous data acquisition. Time $t = 0$ corresponds to the beginning of the laser pulse.

Experimental results

The top surface of the rods is observed during ignition and combustion using the 2D single-band pyrometer, and the temperature on a 1 mm diameter spot at the center of the rod is measured using the spectral pyrometer.

In all the tests presented, the combustion remains located in a small volume of liquid, on the top of the rod. During the combustion process, the volume of liquid may eventually fall down along the rod, but this case is not described here.

Video observations of the mixing of two phases

The combustion process was observed from the point of initial laser heating of the solid surface until self-sustained downward combustion was achieved or the combustion spontaneously extinguished. The video observations show that the combustion process taking place during laser heating can be divided into four steps (Fig. 2):

Step 1.: The ignition of iron—understood as the onset of an accelerated heating of the system caused by a substantial acceleration of the oxidation rate—is described in detail in [19]. It occurs when the surface begins to melt. The thin liquid layer progressively extends to the whole surface of the rod, and then reaches the edges (Fig. 2a).

Step 2.: Fig. 2(a) shows that, when the liquid reaches the edges and when the layer becomes thicker, small darker liquid phases form and then detach from the sides. These darker spots are distinct phases at first and then progressively mix with the lighter phase as they are pushed toward the center by convective movements.

Step 3.: Then dark liquid rises up at different points on the surface, mixing in the brighter liquid.

Step 4.: If the laser power is high enough, a fourth stage is observed where the brightness of the surface becomes homogeneous and vapor appears above the surface.

Temperature and emissivity measurements

A correlation can be made between surface temperatures measured by the spectral pyrometer (Fig. 3a, b, c) and video observations. As described in [20], the spectral pyrometer provides temperature measurements independent from unexpected variations of the emissivity during the observed process and allows a rough evaluation of the local emissivity during the process.

Contrary to the case of pure unoxidized material with constant emissivity (see [20]), the emissivity of the surface fluctuates between 0.5 and 0.8 during the steps I to III and even after the end of the laser pulse and levels off around 0.7 only after 50–100 ms after the end of the laser pulse (Fig. 3a).

The large variations in the emissivity correspond to video pictures showing the surface of the liquid with dark zones and brighter zones mixing. The spatial (1 mm) as well as the temporal (500 Hz) specifications of our spectral pyrometer are obviously insufficient to resolve the movements of the dark and bright zones in the melt. However, the fluctuations, when correlated with the films, give interesting qualitative indications.

During step I, the emissivity is rather high (≈0.8) and decreases at the onset of step II, when the darker liquid begins to move toward the center of the melt, i.e., the observation zone of the pyrometer. Emissivity remains rather high (0.6–0.75) during step II as long as the dark spots remain on the edge (outside the measuring zone). The transition of the heating rate from step I to step II (open circles in Fig. 4a) occurs at a temperature T_C increasing with laser power, from 2680 to 3300 K (Table 1).

Step III begins when dark liquid comes to the surface from all parts of the melt. Then the emissivity of the surface fluctuates from 0.5 to 0.85 as long as inhomogeneities are present on the surface, indicating that these

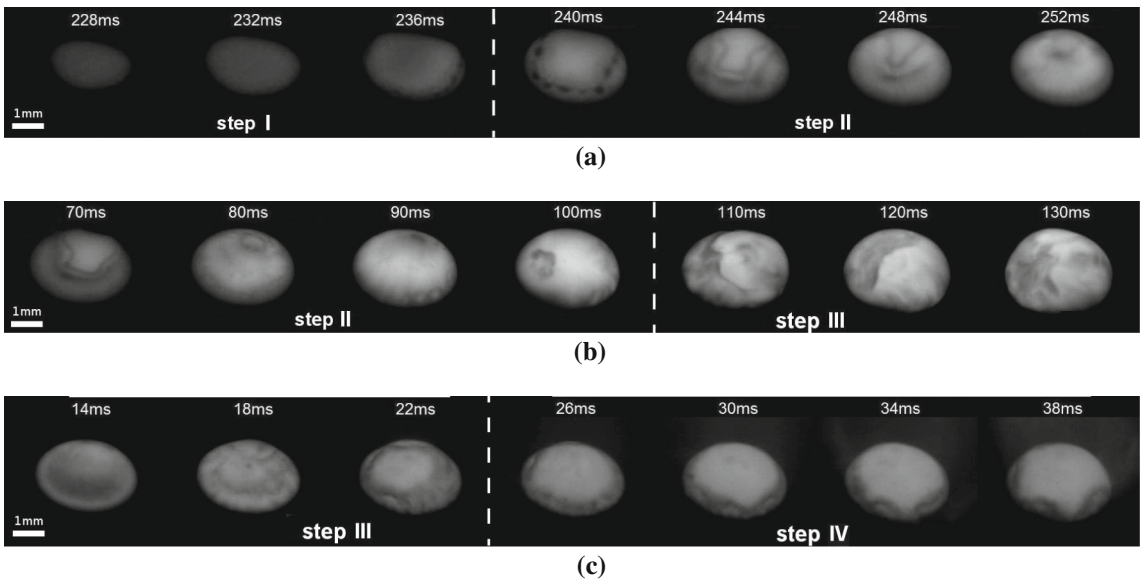

Fig. 2 Infrared images (angle of view 45°) of the *top* of a pure iron rod during laser assisted combustion. **a** From step I to step II ($P = 320\,W$). **b** From step II to step III ($P = 640\,W$). **c** From step III to step IV ($P = 2\,kW$)

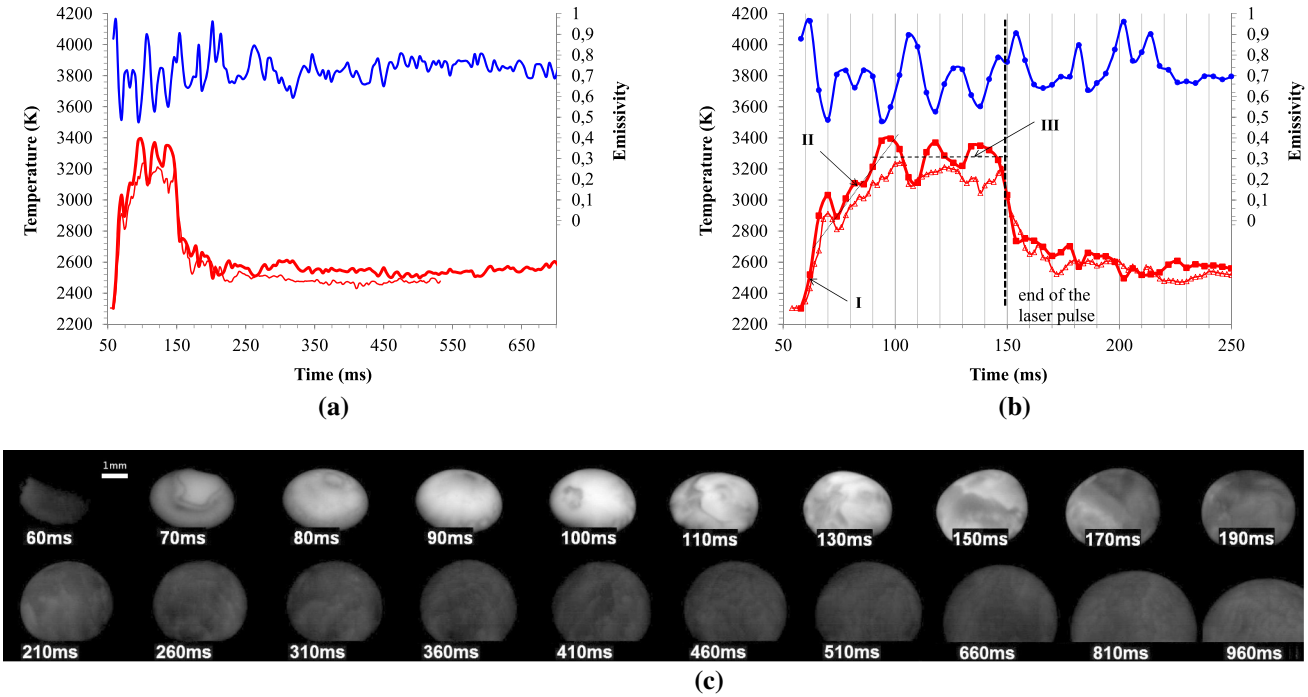

Fig. 3 Temporal evolution of the *top surface* temperature (±60 K) and emissivity (±15 %) of pure iron rods during combustion measured using spectral pyrometry. **a** Temperature and emissivity, laser 640 W–150 ms. **b** Enlargement. **c** Successive frames of the video records (angle of view 45°)

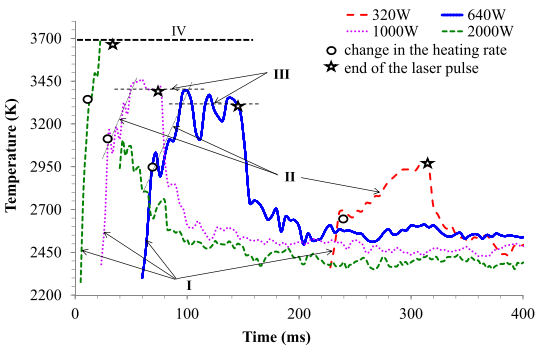

Fig. 4 Temporal evolution of the *top surface* temperature (±60 K) and emissivity (±15 %) of pure iron rods during combustion measured using spectral pyrometry for various laser powers and pulse durations

Table 1 Characteristic temperatures T_c and T_s for various laser powers during combustion

P (W)	T_c (K)	T_s (K)
320	2680	–
640	2900	3300
1000	3150	3400
1500	3240	3620
2000	3300	–

inhomogeneities are due to emissivity and thus to composition gradients being more than temperature gradients. At the same time, the temperature levels off during step III at the saturation temperature T_S increasing with laser power (Table 1).

After the end of the laser pulse, the temperature decreases down to a temperature of approximately 2400 K, at which combustion goes on in an autonomous way. As the melt surface cools down, the surface brightness becomes more and more homogeneous and the emissivity levels off between 0.7 and 0.8.

Very similar behavior is observed for all the laser powers used for ignition. Fig. 4 shows the temperature measurements (spectral pyrometer) made for various laser powers.

The three steps are observed in all cases, except for 2 kW, for which the laser power is high enough to heat the surface of the melt up to the dissociation point of iron oxide (3750 K). At this point, the pyrometer does not provide a reliable value of the temperature because the spectrum is strongly affected by the light bands emitted by the vapor.

Miscibility temperature threshold

The video frames recorded with the 2D pyrometer (Figs. 3c, 5) show variations of the brightness on the surface of the melt during combustion. As explained in [20], these variations may be due either to variation of the temperature or to variation of the emissivity of the liquid.

A careful observation of the surface shows that, depending on the moment of the laser irradiation, two cases may arise.

In one case, one sees two different immiscible phases. One phase, brighter, floats upon another darker phase (as, for example, in Fig. 5a, b at $t = 30$–50 ms, Fig. 5c at $t = 34$–52 ms, Fig. 5b at $t = 140$ ms and Fig. 5c at $t = 124$ ms). A high interfacial tension seems to prevent any mixing to occur between them.

In the other case, two phases are seen, but the interfacial tension between them seems to be reduced so that the phases tend to mix as the convection movements in the melt take place (as, for example, in Fig. 5a at $t = 70$–130 ms, Fig. 5b at $t = 60$–120 ms, and Fig. 5c at $t = 70$–106 ms).

An intermediate case is sometimes observed, as in Fig. 5c, at $t = 106$ ms, where the edges between L1 and L2 are blurred, or in Fig. 5b, at $t = 40$ ms, where the phases remain distinct, but fingering instabilities are visible at the boundary between unoxidized iron and iron oxide, where the darker phase diffuses into the brighter upper phase.

We showed using spectral pyrometry that the darker phases were not only cooler phases, but that their emissivity was also smaller [20]. The emissivity of the darker phase is approximately 0.4, in agreement with the value of 0.35 reported in [14] for pure iron, whereas it is 0.7 for the brighter phase. These measurements allow identifying legitimately the dark and the bright phases to the L1 (unoxidized liquid iron) and L2 (liquid iron oxide) phases of the Fe–O phase diagram, respectively.

Assuming that the bright and dark phases are L2 and L1 phases respectively, with emissivity of 0.7 [20] and 0.35 [14], a systematic measurement of the temperature of adjacent L1/L2 phases was performed on three video frames. The results obtained for the frames of Fig. 5a–c are presented in Table 2 and Fig. 6.

The couple of points on which the measurements are made is very close to each other (<100 microns), and a strong temperature gradient between them is highly unlikely. The assumption is made that the brightness variation between the two close points is only due to emissivity and not to temperature variations because of the size of the observed zones and the relatively high conductivity of the liquids. To test the validity of this assumption, we plot on the same graph the temperatures

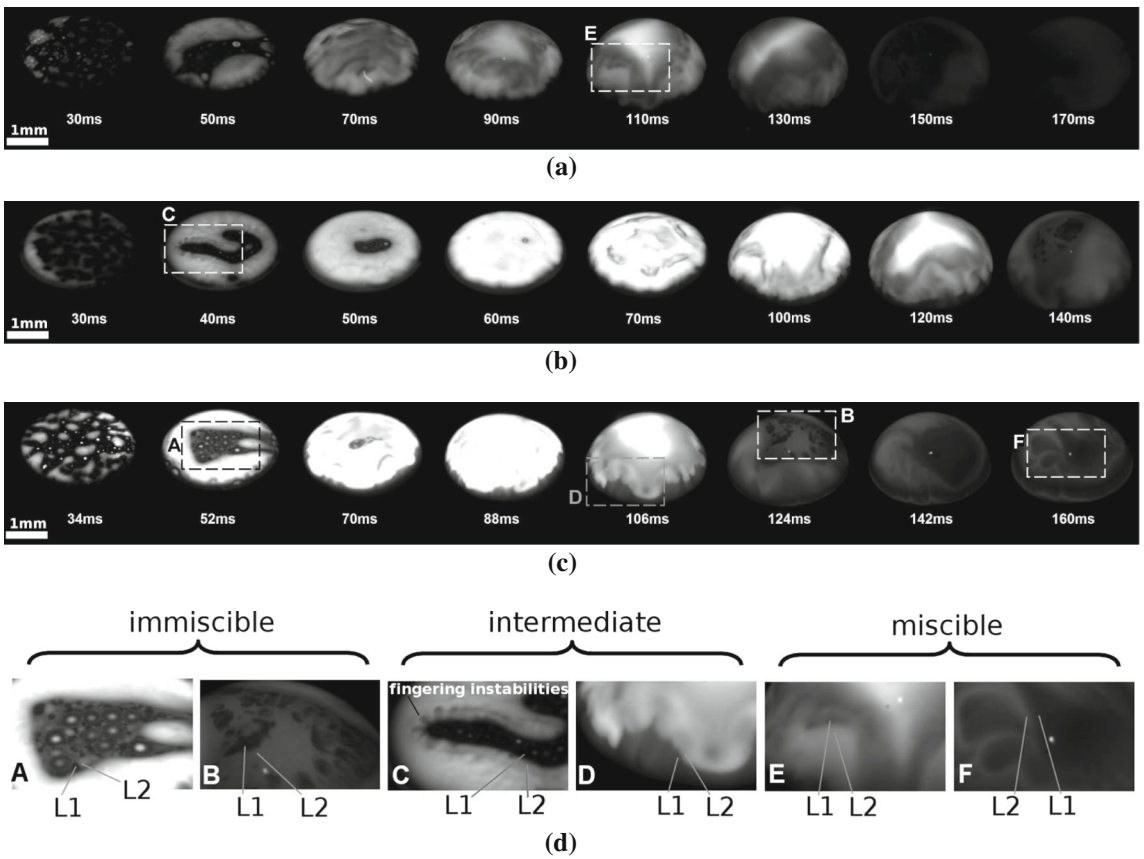

Fig. 5 Video frames of the combustion of pure iron rods recorded using the 2D pyrometer (angle of view 45°), with different shutter speeds of the camera (temperature range). The power and pulse durations of the laser ignition pulse are under each figure. On the *zoomed views*, examples of the location for the temperature measurement for L1 and L2 phase, when L1 and L2 were considered immiscible, miscible, or when the miscibility was partial. **a** 1 kW–130 ms. **b** 1 kW–120 ms. **c** 1 kW– 105 ms. **d** zoomed views

Table 2 Temperatures measured on 2D pyrometer video frames (±30 K). (I: L1 and L2 do not mix; M: L1 and L2 mix.)

1 kW–130 ms					1 kW–120 ms					1 kW–105 ms				
	I		M			I		M			I		M	
t (ms)	L1	L2	L1	L2	*t* (ms)	L1	L2	L1	L2	*t* (ms)	L1	L2	L1	L2
50	2329	2316	–	–	40	2190	2124	2617	2534	50	2288	2191	–	–
70	–	–	2701	2760	50	2263	2288	–	–	106	–	–	2373	2364
110	–	–	2456	2453	100	–	–	2420	2438	124	2029	1993	–	–
150	2329	2233	–	–	120	–	–	2594	2524	–	–	–	–	–
–	–	–	–	–	140	2223	2203	–	–	–	–	–	–	–

of two close points with very significant brightness variations and calculate the temperature of each of them assuming that the dark phase is L1 with a low emissivity (0.35) and the bright phase is L2 with a high emissivity (0.7). The case where the interfacial tension between the dark and bright phases seems to almost disappear is marked by the normal symbols, and the cases where the interfacial tension remains high are marked by bold symbols. If the assumption is correct, each point of the couple must have the same temperature.

This outcome is very clearly achieved considering that the temperatures of the pairs of points on the graph of Fig. 6 are very close from each other. For each point on the graph the temperature that would be obtained if we had made the opposite assumption on the emissivity of the observed point (for L1 supposed phase (dark area), we took 0.7 instead of 0.35, and for L2 supposed phase (bright area), we took 0.35 instead of 0.7) is represented as error bars. The temperatures of the couples of spots are then completely different.

The temperatures represented on the graph of Fig. 6 clearly show that there is a temperature threshold of about 2350 K above which the interfacial tension between L1 and L2 disappears, and the miscibility between L1 and L2 is achieved. It is interesting to notice that the mixing process is reversible. In Fig. 5c, one sees that L1 and L2 mix until $t = 106$ ms, but as the liquid cools down, the L1 and L2 phases dissociate: the surface appear as bright phases (L2) floating over a darker phase (L1) underneath at $t = 124$ ms.

Cooling and gas release

When the laser stops and the temperature begins to decrease toward extinguishment, a strong boil of the liquid is observed until complete solidification of iron oxide (Fig. 7). This is particularly strong for large volumes of the liquid burning during a long time before extinguishment. Many gas bubbles of various sizes can also be seen on the cross sections (Fig. 8).

Metallurgical cuts

The EDS (Energy Dispersive X-ray Spectroscopy) analysis of the samples shows only two distinct possible compositions in all the samples: the first one is pure iron, with no oxygen, and the second one is iron oxide, with no measurable oxygen gradient inside. A Raman analysis shows that the oxide phase is exclusively composed of magnetite Fe_3O_4.

For all the pure iron rods quenched by contact with a copper plate at the bottom of the sample, a clear separation exists between the resolidified unoxidized iron and the iron oxide phases (Figs. 8, 9). However, in several cases, when the cooling was fast enough, the shape of the metal–oxide interface is not flat but irregular (Fig. 8b).

Most of the resolidified iron oxide contains many porosities, the size of which ranges from several microns to several millimeters. These porosities are visible in all parts of the oxide, except on the external parts (Fig. 8a), near the gas–oxide interface and in some places near the metal–oxide interface (Figs. 8a and 9d).

When the melt located near the melting interface has been quenched rapidly enough, the iron oxide has almost no porosities but is peppered with unreacted iron inclusions that seem to have exsolved from the melt during quenching (Fig. 8d).

Discussion

Composition of the melt

The iron–oxygen phase diagram at temperature below 2000 K (see Fig. 10) mentions two possible liquid phases L1 and L2, allowing a relatively narrow range of oxygen content, from 0 to approximately 0.2 w% at 1830 K for the L1 phase, and from 22.7 to 26 w% at the same temperature for the L2 phase.

Information concerning the composition of the melt during combustion can hardly be obtained from metallographic

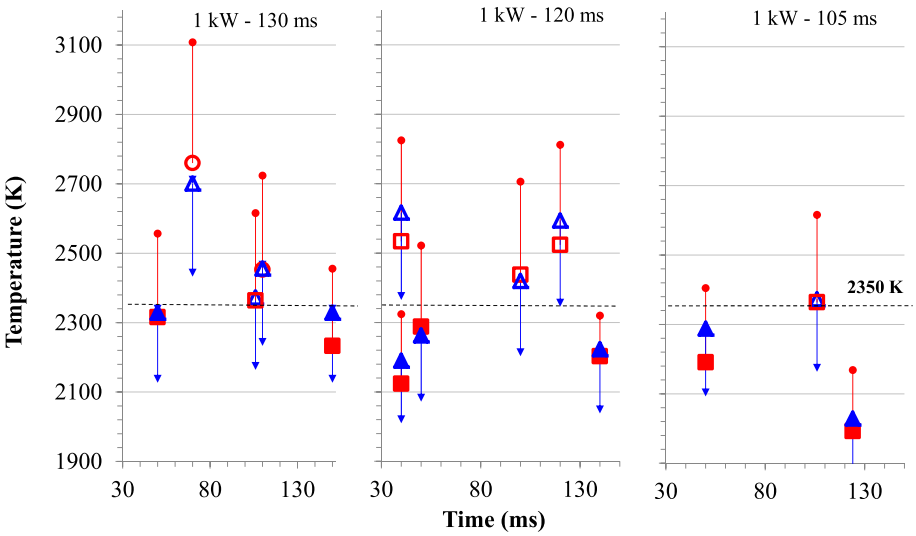

Fig. 6 Temperatures measured on 2D pyrometer video frames. *triangle* and *square* symbols represent, respectively, the temperature of suspected L1 and L2 adjacent phases on the surface of the melt. *Filled symbols* are used when the two phases are immiscible and *open symbols* when they are mixed. The *three graphs* are for measurement on video sequences of Fig. 5a, b, and c. *Error bars* indicate the temperature that would correspond to the same brightness for a low emissivity (0.35) in case of suspected L2 or for a high emissivity (0.7) in case of suspected L1

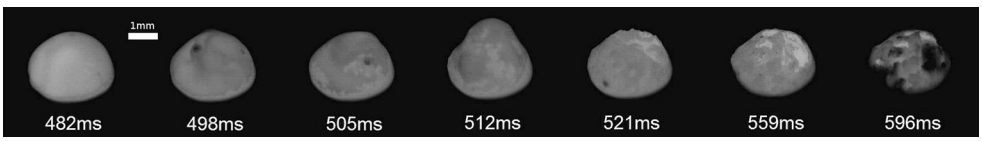

Fig. 7 Cooling liquid oxide melt on the top of a pure iron rod (P(angle of view 45°), laser initiation: 320 W–300 ms) - An oxygen bubble is about to burst at $t = 512\,ms$

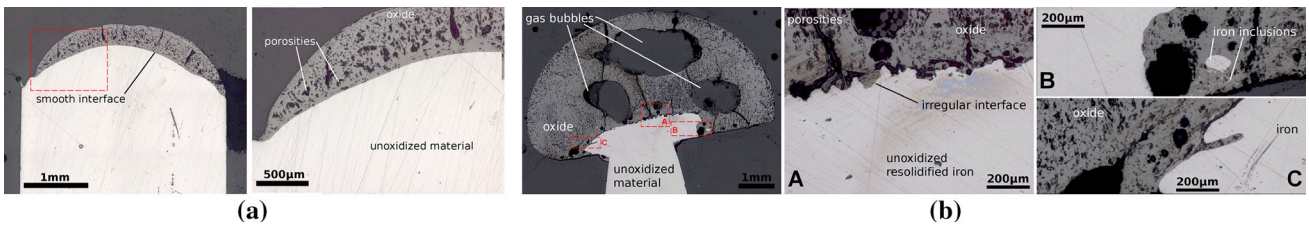

Fig. 8 Cross sections of pure iron sample **a** after slow spontaneous extinction, **b** after propagated combustion, quickly extinguished by contact on a copper plate

analysis of the cross sections of quenched sample, as phase changes occur during cooling, but useful information can nevertheless be obtained.

Excess oxygen in the L2 phase Considering the purity of the iron samples, it can be stated that the liquid observed with the camera as well as the solid material observed on the cross sections contains only iron and oxygen. The boil occurring in the melt during cooling must then be O_2 gas, released as the phase change takes place.

Steinberg et al. [31] as well as Dreizin [5] observed similar outgassing of the melt while cooling, and they concluded that the oxide melt must contain "excess oxygen" compared to the oxygen required to form magnetite.

Indeed, data of the phase diagram (Fig. 10) indicate that only liquid iron with an oxygen content in the melt greater than 28.5 w% can undergo outgassing while cooling. However, the usual phase diagram does not give information as to possible oxygen content in the liquid iron–oxygen melt above 1900 K.

As no boil is observed in the melt at high temperature, we can deduce that a stable liquid phase containing this excess oxygen exists at higher temperature, and that a phase change line must exist (dotted lines in the right part of Fig. 10) within the area of the range of oxygen content from 28.5 w% and above at temperatures greater than 1900 K. As the liquid melt contains far more oxygen than

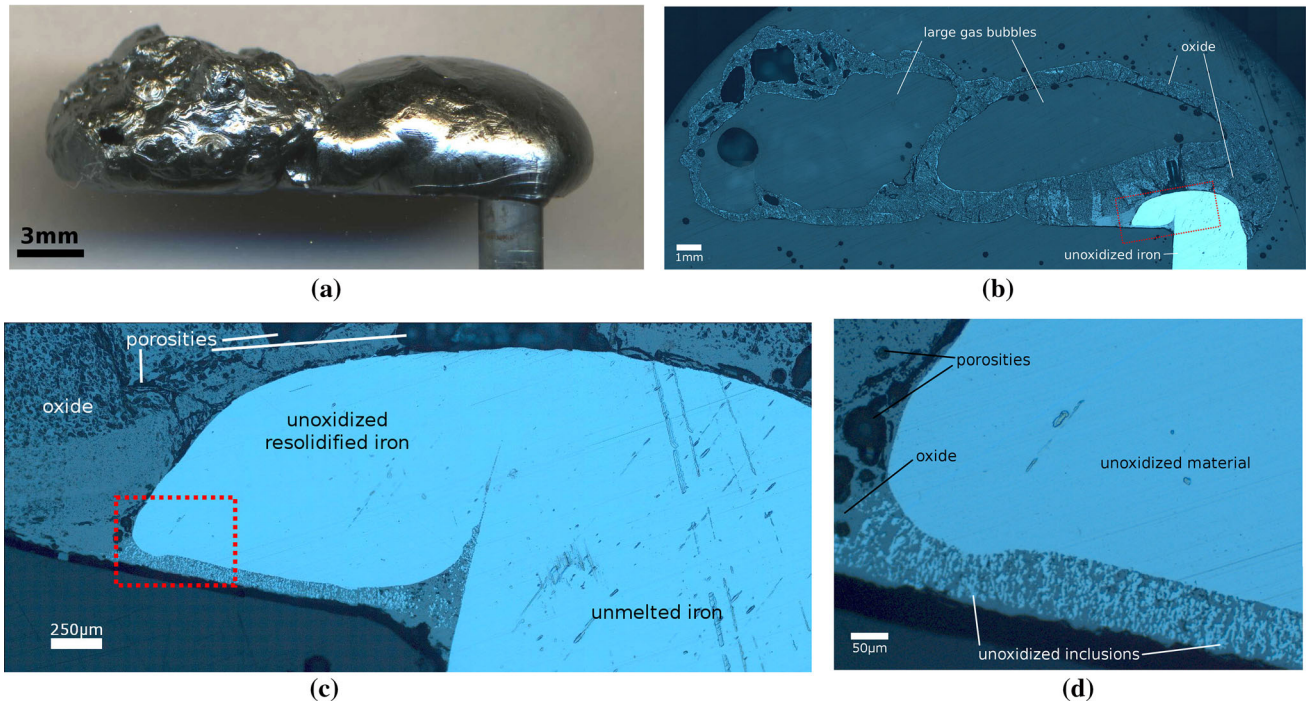

Fig. 9 **a** Pure iron sample quenched by contact on a copper plate; **b** cross sections; **c** and **d** enlarged view of (**b** and **c**)

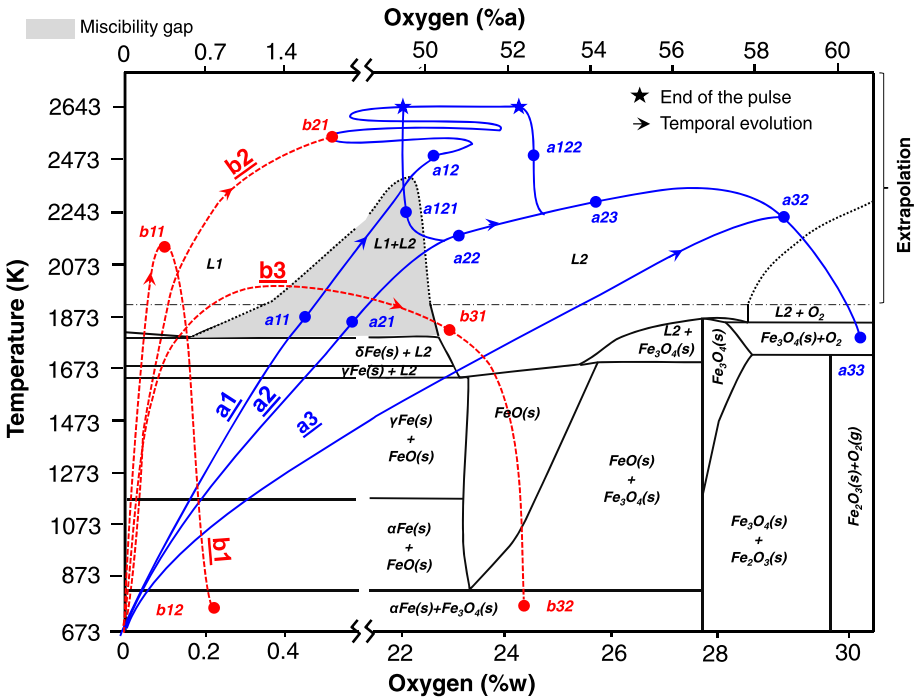

Fig. 10 Iron–oxygen binary phase diagram at atmospheric pressure, from [24], with proposition of extrapolations at higher temperature. The *curves* give the possible evolution (from left to right) of the composition of the surface melt (*blue*) and of the melt close to the melting interface during combustion (*red*) (Color figure online)

required to form magnetite, O_2 gas bubbles form in the melt while cooling and are caught in the solid phase.

Continuity in the oxygen content of the melt According to the phase diagram, the material located at the bottom of the sample, where unoxidized iron inclusions are caught in magnetite (Fig. 9c, d), must result from the solidification of liquid material containing 0 to 27.6 w% of oxygen. Considering the proportion of iron and oxide inclusions, it must have been a L2 phase. This amount of oxygen is normally lower than that required to form hematite alone, this is why inclusions of pure iron are exsolving during solidification.

The smooth transition between these areas on the cross section with the area containing outgassing bubbles shows that a continuity in the oxygen content must have existed in the external part of the liquid melt during combustion, which must have formed one unique phase with variable oxygen concentration, from 23 w% to excess oxygen.

The phase diagram below 800 K indicates that, for an oxygen content below 27.5 w%, only magnetite and α-iron form. If there were a gradient in the composition of all the melt from the melting interface to the gas–liquid interface, the cross section would show only an iron phase peppered with progressively increasing concentration of magnetite inclusions. On the contrary, the straight line between the oxide peppered with iron inclusions and the unreacted iron indicates that, before the solidification occurred, there were two distinct, immiscible phases.

The unreacted iron must have been a L1 phase, and the oxide with iron inclusions together with the oxide with porosities must have been a L2 phase containing from 0 to 27.7 w% oxygen.

Miscibility and immiscibility of the liquid phases

Below 1900 K, the phase diagram of the iron-oxygen system mentions no possibility of mixing between L1 and L2. However, almost no information is available above these temperatures.

As described in Fig. 3, the video observations of the surface and the temperature measurements show inhomogeneities in the brightness at the surface in the melt when the temperature exceeds 2350 K .

The emissivity and temperature measurements indicate that these inhomogeneities are due to composition gradients being more than temperature gradients, and that the L1 and L2 phases get mixed when the liquid reaches a certain temperature threshold.

At the same time that mixing is visible on the surface, the heating rate of the surface decreases, as a result of the addition of fresh metal from the depth of the melt to the surface.

The observation of the cross sections in Fig. 8a supports the fact that, at some point, the interfacial tension between the L1 and L2 phases must have been very low. The shape of the metal–oxide interface is indeed very irregular, and, at some places, oxide inclusions are even caught into iron (Fig. 8b).

The fact that the temperature T_C at which transition from step I to step II occurs is not the same for all the laser powers used to heat the rod suggests that the condition required for this mixing to occur is the attainment of a temperature of the liquid *inside* the melt, more precisely at the interface between the liquid oxide layer (L2) and the unoxidized pure iron melt (L1). Indeed, the temperature gradient between the surface and the core of the melt is greater for high laser power.

Two different processes could explain the mixing of the L1 and L2 phases: the reduction of the interfacial tension between them, leading to a spontaneous emulsification of the phases and the reduction of the miscibility gap when the temperature increases.

Reduction of interfacial tension Riboud et al. [7, 25] showed, in their study on the reactions between slags of various compositions and iron alloys containing aluminum, silicon, phosphorus, boron, or chromium, that a considerable decrease of the interfacial tension occurs when a reaction or a flux of solutes takes place at the interface.

They identified oxygen as the main element involved in this mass transfer, and estimated that the phenomenon is observed when the oxygen flux is larger than 10^{-1} atom/(m^2 s).

Indeed, the interfacial tension between liquid steel or iron and slag depends on the oxygen activity on the interface, which can be increased either by a high oxygen content in iron [21] or by a higher FeO content in the slag (or oxygen in any form) [13, 21, 34].

Spontaneous emulsification Chung et al. [1] also observed a decrease in the apparent interfacial tension to less than 0.1 Nm^{-1} between a Fe–3.28 %Al melt and a CaO–SiO_2–Al_2O_3 slag and considered that the reaction between an element in the alloy and the slag is responsible for this phenomenon. They showed that this decrease of the interfacial tension could even lead to spontaneous emulsification of the immiscible phases.

If the interfacial tension becomes low enough, the dispersion of one phase into another becomes indeed extremely easy. Chung et al. proposed an explanation for this emulsification phenomenon based on the combined effect of the low interfacial tension and the presence of Marangoni convection caused by small gradients of the surface tension due to local reactions [2, 17]. The difference in the fluid flows in each phases across the interface would give rise to a Kelvin-Helmholtz instability, which grows and eventually becomes unstable, leading to spontaneous emulsification.

Even if the typical characteristic times for the dynamic phenomena observed by Riboud et al. [25] and Chung et al. [1] are quite long (several minutes) compared to ours, all the conditions are fullfiled during iron combustion to induce a strong decrease of the interfacial tension between the L1 and L2 layers, and eventually their spontaneous emulsification:

- The L2 phase has a high oxygen content (excess oxygen), and the diffusion coefficient in this ionic melt is considerably increased.
- Without any alloying element, liquid iron can contain up to 2 % oxygen at 2319 K and atmospheric pressure [30].

– The large amount of excess oxygen in the L2 phase may react at the interface with iron of the L1 phase, resulting in a high mass transfer rate across the L1/L2 interface. This effect is considerably enhanced at high temperature.
– The high temperature increases the reaction rates and the diffusion coefficient.
– The exothermal combustion reaction between iron and oxygen induces temperature gradients that, together with the strong composition gradients, lead to Marangoni flows around the interface.

Reduction of the miscibility gap Moreover, the work of Ohtani et al. [22], based on the results of Fischer and Schumacher [6] and their own results, shows that FeO is extensively soluble in liquid iron at 2773 K, so that solubility of oxygen in iron in the L1 phase can reach very high levels, and that complete miscibility between L1 and L2 is even probably achieved above 3073 K. The corresponding additions on the phase diagram of the iron-oxygen system have been made (dotted lines on the left part of Fig. 10).

Our work shows that, at approximately 2350 K, a transition occurs and L1 and L2 begin to mix, whereas at below 2350 K, they remain distinct. The extension of the solubility of oxygen in the L1 phase, together with the spontaneous emulsification due to the reduction of the interfacial tension, results in the mixing of the L1 and L2 phases.

This mixing is likely to lead to considerable increase in the reaction interface area and to change the conditions of oxygen transfer; it should therefore be taken into account in a model of the combustion of iron in liquid phase.

A comprehensive description of the static combustion process based on the phase diagram

Phenomenological description Fig. 11 shows the successive steps (defined above) undergone by the burning rod ("Temperature and emissivity measurements" section) and the corresponding configuration of the L1 and L2 phases during combustion.

Step I corresponds to a very fast oxidation process of the L1 surface, leading to formation of a thin L2 phase on the surface. The formation of a L2 layer on the surface may occur either on the whole surface (slow irradiation) or as a disrupted layer, or L2 spots over a L1 layer (fast irradiation).

When the temperature of the liquid increases, heated by both laser and heat release due to oxidation, the diffusion rate of oxygen as well as the oxygen transfer across the interface between L1 and L2 increases. As temperature and oxygen enrichment increase, the interfacial tension between the L1 and L2 phases thus decreases to the point where the spontaneous emulsification of L1 and L2 becomes possible at the interface (dotted line at step II), resulting in the formation of dark (L1) pure iron drops of liquid detaching from the edges.

After that, two cases can occur, depending on the maximum temperature reached on the surface of the liquid.

In the first case, the transition from step II to step III occurs when the miscibility gap between L1 and L2 is overcome, i.e., when the temperature exceeds 2350 K. At step III, the miscibility between L1 and L2, as well as the onset of large scale Marangoni flows, caused by the temperature gradients (mainly due to laser heating) then results in the global mixing of the phases in all the liquid layer that reaches 2350 K or more. After that, if the laser keeps on heating the surface, the dissociation point of liquid iron oxide is reached at 3650 K and a vapor forms above the surface (step IV). If the temperature inside the melt, at the interface between L1 and L2 exceeds 2350 K, a layer exists between them where L1 and L2 mix.

In the second case, after step II, if the heating rate is low enough (for example, after the end of the laser pulse), and that the surface temperature does not reach 2350 K, spontaneous emulsification may still occur at the interface, but the L1 and L2 layers remain distinct and convective flow may occur only inside each of them (step IIIbis).

Scenarios as paths on the phase diagram Based on the above-described phenomena in the iron-oxygen system, we completed the description of the phase diagram at higher temperatures (Fig. 10).

A description of the combustion process of iron induced by laser can be attempted based on the evolution of the temperature and the composition of the melt.

Fig. 10 presents different possible scenarios for various heating rates of the surface by the laser and for different depths inside the melt. The curves from a1 to a3 are three possible evolution paths of the composition and temperature of the melt at the surface; curves b1 and b2 stand for the liquid closer to the melting interface.

If the laser power is high, the liquid at the surface quickly reaches a high temperature and oxidizes simultaneously (a1 and a2).

If the laser power is high enough, the whole surface does not have the time to oxidize completely, and L2 phases can been seen floating above the L1 phase (a11 and a21, Fig. 5a–c, at the beginning), until the surface is completely covered by the L2 phase (a22, Fig. 5b at 60 ms). If the surface is heated by the laser at such rate that the surface temperature exceeds 2350 K (above the miscibility gap), the L2 phase and the L1 phase underneath begin to mix and the surface shows black liquid arising and mixing simultaneously at the surface (a12, Fig. 5b at $t = 70$ ms). The composition at the surface may then vary, as well as the temperature, as the surface is continuously provided with fresh unreacted metal. If the laser stops, the temperature

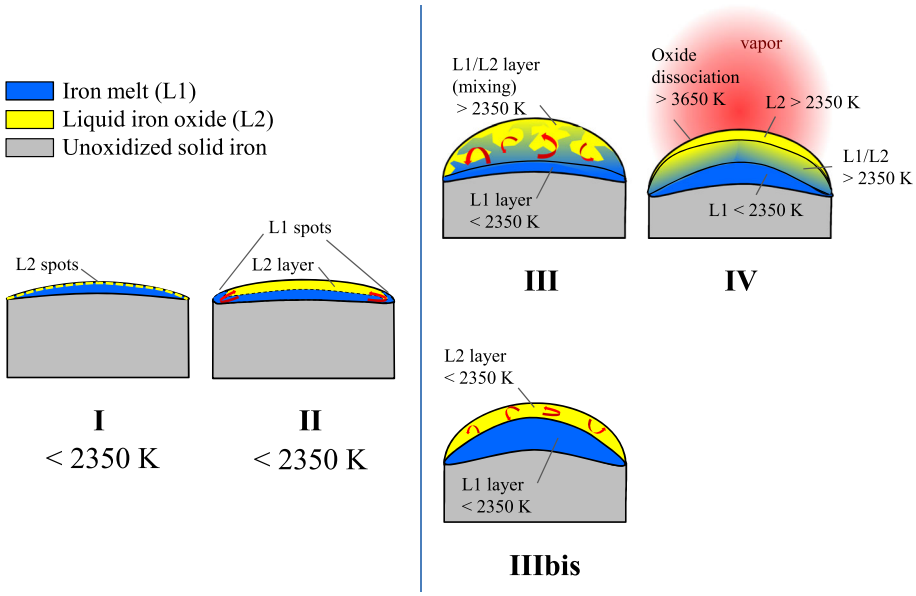

Fig. 11 Section diagram of pure iron rods undergoing static combustion during laser heating in the case where part of the liquid reaches a temperature above 2350 K (*up*) or where temperature remains below 2350 K (*down*) (Roman numerals stand for reaction steps)

will then tend to decrease. When the temperature of the surface of the melt falls below 2350 K depending on the composition of the liquid on the surface, the liquid may either separate into two phases L1 and L2, each covering part of the surface (a121, in Fig. 5c at $t = 124$ ms), or, if the oxygen content is high enough, become a L2 phase covering the whole surface (a122, Fig. 3c after 150 ms). Both cases join the a2 curve after the end of the laser pulse.

If the surface is heated at a slower rate (a21) or if the L2 phase covering the surface is cooling down (a12), the miscibility gap is not exceeded, and the L2 phase floating on the L1 phase surface will progressively extend to cover the whole surface (a22). The brightness of the surface becomes then more and more homogeneous as the oxygen content in the liquid progressively increases (a23). The oxygen content becomes eventually higher than necessary to form Fe_3O_4 (excess oxygen) (a32, Fig. 7 at 482 ms). Then, if the heat release due to combustion is smaller than the heat losses, then the melt cools down and the oxygen is released as bubbles (a33, Fig. 7 from 498 to 520 ms) that are caught in solid magnetite.

A third case is theoretically possible but has not been observed in our experiments. It is represented on curve a3. This case would occur when the metal is heated at a very slow rate. The surface of the metal oxidizes slowly in solid phase (mostly FeO). Then the oxide melts to form a homogeneous L2 phase at the surface. The oxidation reaction heats up the surface and the oxide content increases progressively in the liquid so that the curve eventually merges with the a2 curve (a32).

Now if we consider the phase changes *inside* the melt, three different paths may be followed. If a point very close to the melting interface is considered (b1), L1 is formed when iron reaches its melting point (b11). Few oxygen diffuses at this depth and the liquid does not oxidize much. If cooling occurs, the L1 phase will resolidify as almost pure iron (b12).

In case we consider a point located inside the L1 layer, closer to the L1/L2 interface, if the liquid is heated fast enough (b2), the miscibility gap may be exceeded, and the L1 phase will mix with the L2 phase above (b21).

The third case (b3) occurs when the miscibility gap is not exceeded, but when the progressive oxidation of the melt and the oxygen enrichment at the interface result in spontaneous emulsification of L1 and L2 phases. The mixing between the phases is increased, as well as the oxidation rate. The L1 phase oxidizes to form L2 phase (b31), that will cool down, forming both iron and magnetite from a homogeneous L2 melt (b32, as in Fig. 9d).

Conclusions

In this article, the laser-initiated combustion of pure iron rods has been investigated, using optical pyrometry, video observations, and analysis of metallographic cross sections of quenched burning liquid on copper plates.

The evolution of the surface temperature during laser initiation of combustion has been found to be divided into three main successive steps corresponding to decreasing heating rates of the surface. The emissivity measurement showed that these temperature variations were accompanied with variations of the composition of the melt.

An analysis of the video recordings together with the temperature measurements also showed that, depending on the surface temperature, two liquid phases can be seen

either distinct and immiscible or mixing together. The temperature of the transition at which this mixing occurs has been found to be around 2350 K.

The analysis of the cross section of the molten material quenched on a copper plate showed that, during combustion, it may happen that the liquid oxide melt forms one unique phase with variable oxygen concentration, from 23 w% to excess oxygen.

Bibliographic data along with our experimental results also allowed proposing an original explanation to the temperature and emissivity variations on the surface of the melt. We suggest that, when temperature and oxygen activities in the melt increase, two phenomena can occur, which lead to a mixing of the phases:

- spontaneous emulsification at the interface, due to the joint action of the decrease in the interfacial tension between L1 and L2 and the presence of local gradients around the interface that induce Marangoni flows.
- reduction of the miscibility gap between L1 and L2 at high temperature.

This mixing process actually leads to considerable increase in the reaction interface area and also changes completely the conditions of oxygen and heat transfer in the melt. It is indeed worth taking it into account in a model of iron combustion.

Eventually, based on the above results, we proposed a description of the phase diagram of the iron-oxygen system at higher temperatures and a description of the combustion process of iron induced by laser, based on the evolution of the temperature and the composition of the melt.

Acknowledgements This work pertains to the French Government program "Investissements d'Avenir" (LABEX INTERACTIFS, reference ANR-11-LABX-0017-01) and was financially supported by Air Liquide. The authors wish to thank Grigori Ermolaev (Khristianovich Institute of Theoretical and Applied Mechanics) for discussions of various issues considered in this paper.

References

1. Chung Y, Cramb A (1998) Direct observation of spontaneous emulsification and associated interfacial phenomena at the slag-steel interface. Philos Trans R Soc Lond Ser A 356(1739):981–993
2. Chung Y, Cramb A (2000) Dynamic and equilibrium interfacial phenomena in liquid steel-slag systems. Metall Mater Trans B 31(5):957–971
3. Distin P, Whiteway S, Masson C (1971) Solubility of oxygen in liquid iron from 1785 degrees to 1960 degrees C—a new technique for study of slag-metal equilibria. Can Metall Q 10(1): 13–18
4. Dreizin E (2000) Phase changes in metal combustion. Prog Energy Combust Sci 26(1):57–78
5. Dreizin E, Suslov A, Trunov M (1993) General trends in metal particles heterogeneous combustion. Combust Sci Technol 90(1–4):79–99
6. Fischer W, Schumacher J (1978) Die sttigungslslichkeit von reineisen an sauerstoff vom schmelzpunkt bis 2046c ermittelt mit dem schwebeschmelzverfahren. Arch Eisenhttenwes 49:431–435
7. Gaye H, Lucas L, Olette M, Riboud P (1984) Metal slag interfacial properties - equilibrium values and dynamic phenomena. Can Metall Q 23(2):179–191 76
8. Glassman I (1993) The combustion phase of burning metals—comment. Combust Flame 93(3):338–342
9. Harrison P, Yoffe A (1961) The burning of metals. Proc R Soc A 26lA:357–370
10. Hirano T, Sato K, Sato Y, Sato J (1983) Prediction of metal fire spread in high pressure oxygen. Combust Sci Technol 32: 137–159
11. Hirano T, Sato Y, Sato K, Sato J (1984) The rate determining process of iron oxidation at combustion in high-pressure oxygen. Oxid Commun 6(1–4):113–124
12. Hirano T, Sato K, Sato J (1985) An analysis of upward fire spread along metal cylinders. J Heat Transf 107:708–710
13. Jung E, Kim W, Sohn I, Min D (2010) A study on the interfacial tension between solid iron and CaO–SiO2–Mo system. J Mater Sci 45(8):2023–2029
14. Krishnan S, Yugawa K, Nordine P (1997) Optical properties of liquid nickel and iron. Phys Rev B 55(13):8201–8206
15. Kubaschewski O, Hopkins B (1962) Oxidation of metals and alloys. Butterworths, London
16. Kurtz J, Vulcan T, Steinberg T (1996) Emission spectra of burning iron in high-pressure oxygen. Combust Flame 104(4):391–400
17. Mills KC, Hondros ED, Li ZS (2005) Interfacial phenomena in high temperature processes. J Mater Sci 40(9–10):2403–2409. doi:10.1007/s10853-005-1966-z
18. Muller M (2013) 'Etude du processus d'initiation par laser de la combustion d'un alliage métallique sous atmosphère d'oxygène. PhD thesis, ENSMA
19. Muller M, El-Rabii H, Fabbro R (2014) Laser ignition of bulk iron, mild steel and stainless steel in oxygen atmospheres. Combust Sci Technol 186(7):953–974
20. Muller M, Fabbro R, El-Rabii H, Hirano K (2012) Temperature measurement of laser heated metals in highly oxidizing environment using 2D single-band and spectral pyrometry. J Laser Appl 24(2):022006
21. Ogino K, Hara S, Miwa T, Kimoto S (1984) The effect of oxygen-content in molten iron on the interfacial-tension between molten iron and slag. Trans Iron Steel Inst Jpn 24(7):522–531
22. Ohtani E, Ringwood A (1984) Composition of the core.2. effect of high-pressure on solubility of feo in molten iron. Earth Planet Sci Lett 71(1):94–103
23. Ohtani H (1990) Theoretical consideration on the ignition of hot iron in high pressure oxygen. Fire Sci Technol (Noda Jpn) 10(1–2):1–9
24. Philibert J, Vignes A, Bréchet Y, Combrade P (2002) Métallurgie—du minerai au matériau. Dunod, Paris
25. Riboud P, Lucas L (1981) Influence of mass transfer upon surface phenomena in iron and steelmaking. Can Metall Q 20(2):199–208
26. Sato J, Hirano T (1986) Behavior of fire spreading along high-temperature mild steel and aluminum cylinders in oxygen. Am Soc Test Mater 910:118–134
27. Sato J, Ohtani H, Hirano T (1995) Ignition process of a heated iron block in high-pressure oxygen atmosphere. Combust Flame 100(3):376–383
28. Sato K, Sato Y, Tsuno T, Tsuno T, Nakamura Y, Hirano T (1982) Metal combustion in high pressure oxygen atmosphere: detailed observation of burning region behaviour by using high-speed photography. In 15th International Congress on High Speed Photography and Photonics, vol 384. p 828–832
29. Steinberg T, Benz F (1991) Iron combustion in microgravity. Am Soc Test Mater 1111:298–312

30. Steinberg T, Kurtz J, Wilson D (1998) The solubility of oxygen in liquid iron oxide during the combustion of iron rods in high-pressure oxygen. Combust Flame 113(1–2):27–37
31. Steinberg T, Mulholland G, Wilson D (1992) The combustion of iron in high-pressure oxygen. Combust Flame 89(2):221–228
32. Steinberg T, Wilson D, Benz F (1992) The combustion phase of burning metals. Combust Flame 91(2):200–208
33. Steinberg T, Wilson D, Benz F (1993) The combustion phase of burning metals—response. Combust Flame 93(3):343–347
34. Sun H (2006) Reaction rates and swelling phenomenon of Fe–C droplets in FeO bearing slag. ISIJ Int 46(11):1560–1569
35. Wilson D, Steinberg T, Stolzfus J (1997) Thermodynamics and kinetics of burning iron. Am Soc Test Mater 1319:240–257